Conformation-Activated Protonation in Reaction Centers of the Photosynthetic Bacterium *Rhodobacter sphaeroides*†

László Kálmán and Péter Maróti*

Institute of Biophysics, József Attila University Szeged, Egyetem utca 2, Szeged, Hungary H-6722

Received July 31, 1997; Revised Manuscript Received October 2, 1997⊗

ABSTRACT: Kinetics and stoichiometry of proton binding/unbinding induced by intense (1 W cm^{-2}) and continuous illumination were measured in the isolated reaction center (RC) protein from photosynthetic purple bacterium *Rhodobacter sphaeroides* in the absence of an external electron donor. At high ionic strength (100 mM), large proton release (≈6 H^+ per RC) was observed at pH 6 and substoichiometric H^+-ion binding (≈0.3 H^+ per RC) at pH 8. These observations together with optical spectroscopy on the oxidized dimer indicate that, at room temperature, two distinct conformations of the RC can be obtained depending on the pH, E_h, and illumination. Acidic pH, a large redox gap between the actual E_h of the solution and the midpoint potential of the acceptor quinone, and strong illumination favor the conversion of the RC from the dark-adapted state to the light-adapted state. These conformations differ greatly in the rates of primary photochemistry, the reoxidation of semiquinone and the rereduction of the oxidized dimer, and the protonation states of the amino acids of the protein. Whereas substoichiometric proton unbinding is observed in the P^+Q redox state of the protein in the dark-adapted conformation, much larger H^+-ion release is detected in the light-adapted conformation. From the pH dependence of the key processes in the conformational change and reoxidation of semiquinone, we concluded that they are controlled by protonatable groups available in the protein. A simple phenomenological model is presented that relates the rates and equilibrium constants of the electron transfer reactions and the conformational change of the RC.

The light-induced primary charge separation of photosynthesis takes place in the integral membrane protein−pigment complex, the so-called reaction center (RC).[1] The three-dimensional crystal structure of the RC of the purple photosynthetic bacterium from *Rhodobacter sphaeroides* has been determined by X-ray diffraction with resolution limits of 3.7 Å (*1*), 3.0 Å (*2*), 2.8 Å (*3*), and 2.65 Å (*4*). These structures show two sets (A and B) of bacteriochlorophyll (BCL), bacteriopheophytin (BPH), and quinone (Q) cofactors arranged (quasi) symmetrically with respect to a bacteriochlorophyll dimer (P). In contrast to the apparent 2-fold symmetry of the cofactors, the electron and proton transfer are highly asymmetric. Only one of the two branches (A) is active. Upon light absorption, it conducts an electron from the excited singlet state of the dimer (P^*) to Bph_A via the accessory BCL_A in about 3.5 ps (*5*, *6*) and in another 200 ps to the primary quinone, Q_A (*7*). The reduced primary quinone, Q_A^-, then transfers the electron to the secondary quinone, Q_B, within about 100 μs (*8*, *9*), but the rate is a matter of recent debate (*10*). If P^+ is rereduced by an electron donor (soluble cytochrome c_2 *in vivo*), then a second flash induces turnover of the RC, resulting in the double reduction of Q_B to quinol (for review, see refs 11−14).

The electron transfer is accompanied by conformational changes and proton uptake reactions of the RC. Much indirect evidence has been accumulated which favors structural changes linked to light-induced $PQ_A \rightarrow P^+Q_A^-$ charge separation. Significant volume contraction [12−33 Å (mol of photon)$^{-1}$] was reported (*15*−*17*). Kleinfeld et al. (*18*) found that the rate of flash-induced $P^+Q_A^- \rightarrow PQ_A$ recombination at the temperature of liquid nitrogen was 5 times smaller in RCs frozen during continuous illumination than in RCs cooled in the dark. They argued that the light pretreatment caused structural change which increased the electron transfer distance. Kinetically resolved electrogenic (*19*) and electrochromic measurements (*20*, *21*) associated with Q_A reduction nicely demonstrated the mobility of this region of the protein. Brzezinski and Andréasson (*22*) observed that the cleavage of the RC by trypsin was different in the PQ_A and $P^+Q_A^-$ states which indicated protein structural changes after charge separation (*22*). Very recently, a structure was published showing very large changes in the position of Q_B due to the presence of a charge upon illumination (*23*). On the other (periplasmic) side of the RC, two distinct conformations of P^+ were reported that depended on the detergent and the temperature (*24*).

The proton uptake associated with electron transfer in the RC is the primary step in establishing transmembrane proton potential (*25*). The protonation equilibrium between the light-activated RC and the aqueous bulk phase controls at least three major processes: (1) energetic stabilization of

† This study has been supported by grants from the Hungarian Science Foundation (OTKA 17362/95), the Foundation of the Hungarian Ministry of Education (MKM 53205/96/XIV and FKFP 1288/1997), the French and Hungarian Governments (Balaton Project, 7/95), and the International Human Frontier Science Program (RG-329/95 M).

* To whom correspondence should be addressed. Fax: 36-62-454-121. E-mail: pmaroti@physx.u-szeged.hu.

⊗ Abstract published in *Advance ACS Abstracts*, November 1, 1997.

[1] Abbreviations: AQ, anthraquinone; BCL, bacteriochlorophyll; BPH, bacteriopheophytine; DMBQ, 2,5-dimethyl-1,4-benzoquinone; LDAO, *N*,*N*-dimethyldodecylamine *N*-oxide; P, bacteriochlorophyll dimer; PMS, *N*-methylphenazonium methosulfate; Q_A and Q_B, primary and secondary quinone acceptors, respectively; RC, reaction center; TMPD, *N*,*N*,*N*′,*N*′-tetramethyl-*p*-phenylenediamine; Triton X-100, octyl phenol polyethylene glycol ether; UQ_{10}, ubiquinone-50.

S0006-2960(97)01882-5 CCC: $14.00

redox states of the RC involving the semiquinones (*26*−*30*), (2) exportation of a reducing equivalent in the form of quinol (Q_BH_2) from the RC (*31*, *32*), and (3) stabilization of light-induced conformational changes of the RC (*18*, *19*). The stoichiometry of proton uptake for quinol formation is two H^+ ions per RC, and the secondary quinone is directly protonated: $Q_B + 2e^- + 2H^+ \rightarrow Q_BH_2$. The sequence of proton and electron transfer to Q_B has recently been revealed (*33*). In contrast to quinol formation, the establishment of semiquinones (Q_A^- or Q_B^-) upon flash excitation is accompanied by substoichiometric amounts of H^+-ion binding and the targets of protonation are not the semiquinones themselves but the amino acid residues of the protein (*27*, *28*, *34*, *35*). The observed stoichiometry of protons bound per RC depends on the redox states of the cofactors and is decreased by P^+ in the neutral and acidic pH range (*26*, *28*). In the presence of P^+, significant amounts of H^+ binding (>0.1 H^+ per RC) can be expected only in the alkaline pH range. Negative charge on the quinones (positive charge on the dimer) causes pK_a shifts to higher (lower) values for various protonatable residues of the RC. Thus, the proton uptake (release) compensates for the appearance of negative (positive) charge in the protein matrix. Although the electrostatic interaction can have a surprisingly long range (*36*), a minimum of four or five separate acid−base groups were observed to be involved in the proton uptake after a flash with pK_a shifts of 0.5−1.5 pH units (*27*, *34*, *36*, *37*). If no donor was present for P^+ rereduction, the kinetics of proton uptake and the subsequent proton unbinding followed the changes in redox states of the RC due to charge separation ($PQ_A \rightarrow P^+Q_A^-$) and dark recombination ($P^+Q_A^- \rightarrow PQ_A$), respectively (*38*).

These conclusions were drawn mainly from flash-induced proton binding measurements. There are several indications, however, that the protonation may be accompanied by conformational changes of the RC which can make the direct comparison of the short and long term behavior of protonation difficult. The relaxation of the polarizability of the RC in response to $P^+Q_A^-$ is essentially completed in about 1 μs (*39*). Long after establishment of electrostatics in the protein, no equilibria in protonation were observed (*40*). The pH dependence of the redox midpoint potential of the Q_A/Q_A^- couple in isolated RCs determined by equilibrium redox titration (*34*) was about 3 times larger than that predicted from flash-induced proton uptake and delayed fluorescence (*31*). Recent acid−base equilibrium titration of bacterial RCs showed that the majority of protonatable groups do equilibrate with the aqueous bulk through the detergent phase on an extended time scale (*41*). The quantitative disagreements between dielectric continuum calculations and experiments on the stoichiometry of proton uptake called for consideration of additional factors such as conformational changes of the protein or displacement of internal water molecules (*42*−*46*).

In this paper, we present the kinetics and stoichiometry of proton uptake and release of isolated RCs with no external electron donor upon a rectangular shape (unit step) of illumination on a wide time range. These investigations are the extension of earlier experiments with flash excitation (*26*−*28*, *34*) and provide direct information on long term protonation of the RC. The substoichiometric proton uptake was followed by surprisingly large and pH-dependent proton release after prolonged illumination. We interpret the unusual kinetics and stoichiometry to reflect conformation-dependent protonation states of the RC protein.

MATERIALS AND METHODS

RCs from carotenoidless mutants (R-26) of *Rb. sphaeroides* were isolated in LDAO and purified as described earlier (*27*). The purity, defined as the absorbance ratio OD_{280}/OD_{802} was less than 1.30 for all preparations, reflecting a purity of better than 90%. The concentration of the RC was determined from the 802 nm band of the steady state absorption spectrum using an absorption coefficient ϵ^{802} of 318 mM^{-1} cm^{-1} (*29*). After purification, the RC showed little secondary quinone activity which was checked by the flash-induced charge recombination kinetics. In samples with only primary quinone activity, terbutryn, a potent inhibitor of interquinone electron transfer, was routinely present at a concentration of 60 μM (*47*). Removal of native UQ_{10} and substitution by AQ at the Q_A binding site was carried out according to Okamura et al. (*48*) and Liu et al. (*49*). The secondary quinone activity was reconstituted up to 90% by adding a 10-fold excess of UQ_{10} to the RC solution. The ionic detergent (LDAO) was removed and replaced by nonionic detergents (Triton X-100 and dodecyl β-D-maltoside) after a long (48 h) dialysis at 4 °C by frequent changing the dialyzing medium. The Tris buffer content in the experimental sample was about 10 μM, which gave a negligible buffering capacity even at pH 8.0. The sample was kept in an airtight cuvette and was routinely degassed by bubbling nitrogen gas. The assay solution was 100 mM NaCl, 0.03% Triton X-100, and 2−5 μM RC at room temperature.

Light-induced absorbance changes were measured on a spectrophotometer of local design (*27*). A flash bulb (EG&G, model FX-200), a laser diode (Laser Diode, Inc., type LCW-100; emission wavelength of 810 nm, power of 500 mW), or a projection lamp with a heat filter and a mechanical shutter (about 1 W/cm^2 incident intensity) was used for excitation. The redox state of the dimer was followed by the light-induced absorption change at 865 nm where the contribution of redox changes of other cofactors (mainly the quinone) was negligible.

Light-induced protonation of the RC was measured optically, by pH indicator dyes, and electrically, by a pH electrode. The absorbance change of the pH indicator dye (in order of increasing pK, bromocresol purple, phenol red, cresol red, *m*-cresol purple, and *o*-cresol phthalein) was monitored at 586 nm, the isosbestic wavelength of $PQ_A \rightarrow P^+Q_A^-$ transition. The true H^+ binding was the difference of the dye responses in unbuffered and buffered samples. In electric measurements, pH changes upon illumination or addition of titrant were followed by a combined glass electrode (Orion, model 91-03) and pH meter (Orion model 710, precision of 0.1 mV). Potentiometric titration was performed on a concentrated (5−10 μM) solution of RCs with a locally constructed and computer-controlled device (*41*). The titrant solutions (NaOH and $HClO_4$) were prepared and stored under a nitrogen atmosphere.

The redox potential was measured with a platinum electrode versus the Ag/AgCl electrode reference of a combination pH electrode (*50*). The potential of the solution was varied by additions of PMS, DMBQ, TMPD, and ferricyanide redox mediators. All measurements were carried

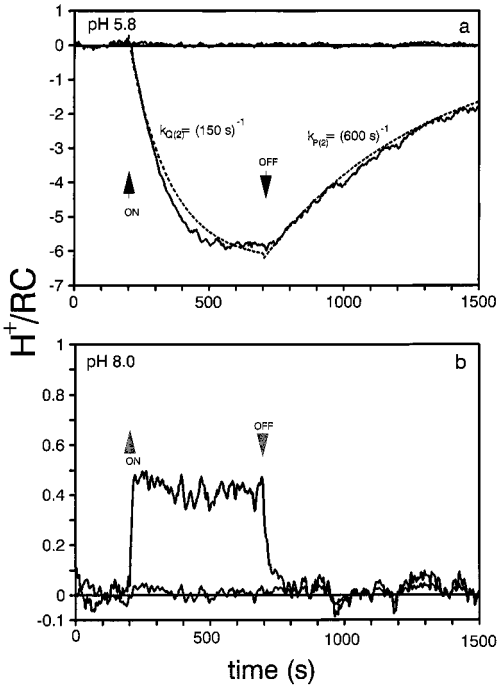

FIGURE 1: Rise and decay of proton release/uptake induced by continuous and strong illumination at pH 5.8 (a) and pH 8.0 (b) in Q_A active RCs from *Rb. sphaeroides* measured by a pH electrode. The H^+ ions were referred to the concentration of photoactive RCs. The signals of buffered samples (background) are also shown. The dashed line was calculated from Scheme 1, where $k_{Q(2)}$ is the rate constant of the semiquinone oxidation in conformation 2 determined from Figure 6a and $k_{P(2)}$ is the rate constant of the decay of the (large proton release) P^+Q_A state in conformation 2 (see also Figure 7b). Conditions were as follows: 3 μM RC, 0.03% Triton X-100, 100 μM terbutryne, 100 mM NaCl, and a 1 W/cm^2 incident light intensity. Mes (10 mM at pH 5.8) and Tris (10 mM at pH 8.0) were used to buffer the sample.

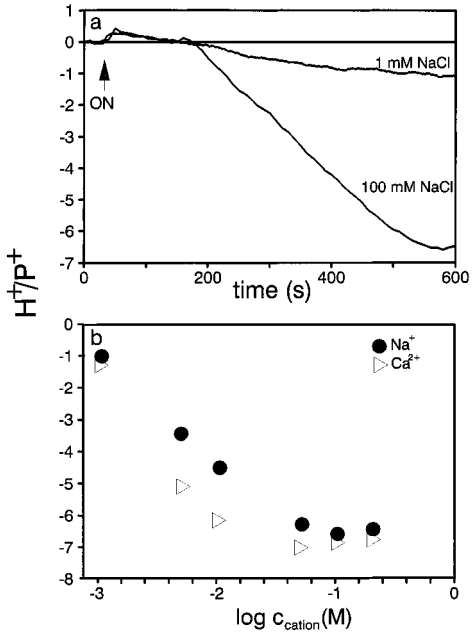

FIGURE 2: Effect of ionic strength on the kinetics (a) and stoichiometry (b) of the proton release in RCs under continuous illumination at pH 6.0 measured by a pH electrode. The concentration of light-induced H^+ ions was referred to that of the oxidized dimer (P^+) and was determined 600 s after the onset of illumination in panel b. Conditions were as in Figure 1, except $CaCl_2$ in panel b.

out at room temperature (T = 295.0 ± 0.5 K) and under anaerobic conditions.

RESULTS

Protonation of RCs under Strong Continuous Illumination. The stoichiometry and kinetics of proton binding/unbinding to RC were measured under continuous and intense (≈1 W cm^{-2}) illumination at slightly acidic and alkaline pH values (Figure 1). The turnover of the RC was inhibited as no external donor was present and the RC showed no secondary quinone activity. Contrary to the expectations from flash-induced H^+ binding experiments (*27*, *28*, *34*), significant proton release was observed at pH 5.8 (Figure 1a). The stoichiometry of proton unbinding was as large as 6 H^+ per RC after several minutes of illumination. At pH 8.0 and under otherwise identical conditions, however, a substoichiometric amount of proton uptake (0.4 H^+ per RC) was measured during illumination (Figure 1b). The buffers (10 mM MES at pH 6.0 and 10 mM TRIS at pH 8.0) eliminated the measured (proton) signal in both cases. The light-induced changes in protonation were reversible as the RC returned to its initial state after (pH-dependent) prolonged dark adaptation.

The kinetics of protonation consisted of several phases. After the onset of the excitation, the traces started at both pH values with an abrupt proton binding which was slowly overlapped by large proton release at pH 6. The proton release occurred in two, kinetically distinct steps; the faster component eliminated the substoichiometric amount of protons bound to the RC right after the onset of the illumination, and the slower component offered large proton release (Figure 2a). The slow phase was found to be very much sensitive to the ionic strength of the solution; proton unbinding stoichiometry significantly larger than 1 H^+ per P^+ could be observed at high ionic strength only. Divalent cations (Ca^{2+}) had a more pronounced effect than monovalent cations (Na^+) (Figure 2b).

Measurements similar to those in Figure 1 were carried out at different pH values in RCs where the secondary quinone activity failed (Q_A active) or was restored (Q_B active). The steady state stoichiometric values of proton binding (+)/unbinding (−) were plotted as function of pH (Figure 3). Independent of the Q_B occupancy, large proton release was observed in the acidic region centered around pH 5.5 which was followed by substoichiometric proton binding around pH 8. The stoichiometry of H^+-ion unbinding was somewhat larger in Q_B active than in Q_A active RCs. In the alkaline range around pH 10, H^+-ion unbinding could be detected in Q_A active RCs and proton binding in Q_B active RCs. A similar difference in proton release after flash excitation was observed in P^+Q_A and P^+Q_B states of the RC (*28*).

The kinetic pattern of protonation/deprotonation depends strongly on the actual redox potential (E_h) of the medium (Figure 4). The more reducing the medium, the smaller the proton release is. At the lowest redox potential (E_h = 110 mV) used in this study, the proton release became comparable to the substoichiometric proton binding and no net protonation could be detected after prolonged illumination (Figure 4a).

A similar pH dependence but kinetics of proton release about 1 order of magnitude faster can be observed if the

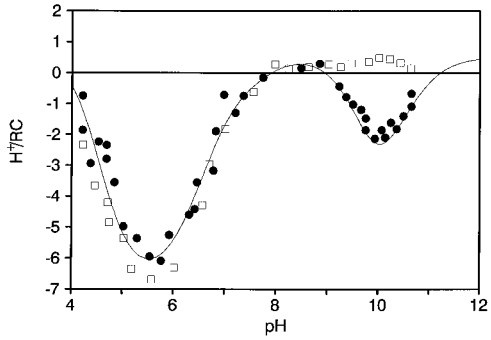

FIGURE 3: pH dependence of light-induced proton release of Q_A (●) and Q_B active (□) RCs measured 600 s after the onset of strong (1 W cm^{-2}) and continuous illumination. The data of Q_A active RCs were approximated by the involvement of six protonatable residues with a pK_{dark1} of 6.8 and a pK_{light1} of 4.8 in the acidic pH range, four ionizable groups with a pK_{dark2} of 10.4 and a pK_{light2} of 9.6 in the alkaline pH region, and 0.3 H^+ per RC proton uptake as background between pH 7.0 and 9.0. The solid line represents the sum of the Henderson−Hasselbalch type titration curves of the protonatable residues. Conditions were as in Figure 1.

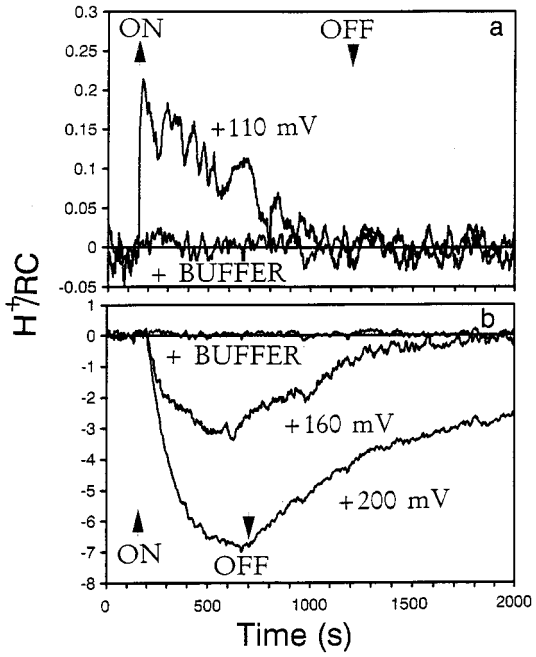

FIGURE 4: Kinetics of light-induced proton binding/unbinding in Q_A active RCs from *Rb. sphaeroides* at pH 6.0 at different *in situ* redox potentials. The stoichiometry of protonation due to continuous and strong illumination was measured by a pH electrode. Conditions were as in Figure 1, except for the mediators: 10 μM PMS (110 mV) and 10 μM PMS and DMBQ, respectively (160 and 200 mV).

native UQ_{10} at the Q_A binding site is replaced by AQ, a low-potential quinone analogue. It is demonstrated at two pH values; large (about 8 H^+ per RC) proton release at pH 6.0 (Figure 5a) and significantly smaller release (about 2 H^+ per RC) at pH 7.7 (Figure 5b) can be detected.

Oxidation and Rereduction Pathways of the Dimer. The kinetics of formation and dark relaxation of the oxidized dimer ($P^+ \rightarrow P$) can be followed by the absorption change at 865 nm. The traces depend on the state of the quinone acceptor complex and the duration of the illumination that formed P^+. Figure 6 demonstrates the kinetics of P^+ in Q_A active RCs with native UQ_{10} at the Q_A site upon the rectangular shape of excitation. The traces show slight temporal changes during illumination and complex decay kinetics in the dark. Shortly after the onset of the illumination, P^+ reaches its maximum value (obtained also by saturating flash excitation), and moves in and out of a shallow (≈5%) dip with $k_c + k_{AP} \approx$ (150 ms)$^{-1}$ and $k_{I(2)} \approx$ (5 s)$^{-1}$ rate constants, respectively. After the illumination was switched off, P^+ shows multiphasic dark relaxation kinetics that depends on the duration of excitation. After very short illumination, all P^+ decays via charge recombination with a k_{AP} of (100 ms)$^{-1}$. After longer and longer illumination,

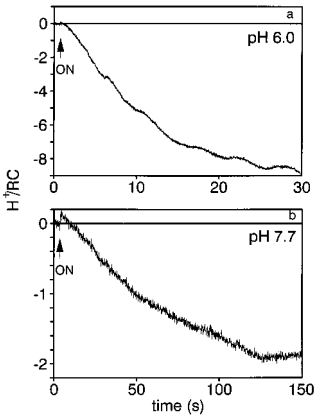

FIGURE 5: Kinetics of proton release in Q_A-substituted RCs of *Rb. sphaeroides* under continuous illumination at pH 6.0 (a) and 7.7 (b). The native UQ_{10} was replaced by low-potential anthraquinone in the Q_A-binding site. Conditions were as follows: 4 μM RC, 0.03% Triton X-100, 100 mM NaCl, and a 1 W cm^{-2} light intensity.

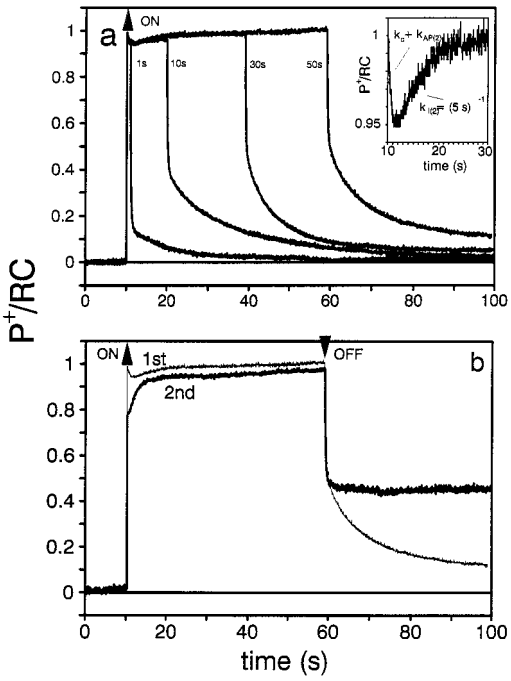

FIGURE 6: Formation and relaxation of the oxidized dimer (P^+) upon first illumination of different durations (a) and first and second illuminations of constant (50 s) duration (b) in Q_A active RCs of *Rb. sphaeroides* at pH 6.0. (a) Times of 1, 10, and 30 s were the durations of the (first) illumination of different samples, and the time constants of the subsequent dark relaxation were 100 ms and 10 and 600 s, attributed to $P^+Q_A^-$(1, 2), P^+Q_A(1), and P^+Q_A(2) states of the RC, respectively (see Scheme 1). The numbers in parentheses refer to the two conformations of the RC. (Inset) Expansion of the initial phase. The rise time of 5 s corresponds to the $PQ_A(2) \rightarrow P^+Q_A^-(2)$ light reaction in the second conformation state of the RC. (b) The second illumination followed the first one after a 600 s dark interval. Conditions were as follows: a 1 W cm^{-2} power of excitation, an 865 nm detection wavelength, 3 μM RC, 0.03% Triton X-100, 100 mM NaCl, and 100 μM terbutryne.

however, two additional (slower) phases with rate constants $k_{P(1)}$ of (10.7 s)$^{-1}$ (slow) and $k_{P(2)}$ of (600 s)$^{-1}$ (very slow) appear with increasing amplitudes. The slow component is established within several tens of seconds of illumination (Figure 6a), and the even longer excitation increases the amplitude of the very slow component (Figures 6b and 7b). The portion of the fast phase remains about 50% after very long excitation. The weight of the slower components in P^+ dark relaxation increases monotonously not only with the duration of the excitation but also with the oxidizing redox potential of the solution (data not shown). If AQ replaces UQ_{10} in the Q_A binding site, the very slow component will dominate the dark decay of P^+ after sustained illumination.

The rate of photooxidation of the dimer (k_I) depends on the preillumination history and pH of the RC. It is well demonstrated if the kinetics of formation and decay of P^+ evoked by the first and second illumination are compared (Figure 6b). Several minutes after the first illumination, all P^+ is rereduced because the second illumination generated about the same amount of P^+ as the first one. Although the intensities of the first and second excitation were equal, the rate of photochemistry during the second illumination became much lower [$k_{I(2)} \approx (5\ s)^{-1}$] in a significant part of the RCs (≈20%). This fraction of the RC remained trapped in a second conformation where the yield of charge separation is much less than that in the completely relaxed (first) conformation of the RC. It is interesting that similar behavior was observed in the kinetics of absorption changes at 645 nm (BPH^-) and 450 nm (Q_A^-) during subsequent illuminations in QA active RCs in the presence of cytochromes (*51*), but their interpretation (accumulation of negative charges on the BPH and Q_A acceptors) cannot be relevant in our case (we had no external donor).

Identification of the Large Proton Release State. Depending on the pH, E_h, and light conditions, a significant portion of oxidized dimers remains trapped in the P^+Q_A state of the RC. The rate constant of dark rereduction of P^+ is larger after flash excitation and at moderately high oxidizing redox potentials (Figure 7a, first conformation) than after strong and continuous illumination (Figure 7b, largely second conformation). The kinetics of very slow accumulation of the long-lived P^+Q state during excitation and its decay in the dark correlate well with the observed protonation/deprotonation of the RC (Figure 1a). Therefore, the high proton release state of the RC may be attributed to the P^+Q redox form of the RC in the second conformation.

Reoxidation of Semiquinone. The light-induced semiquinone can be reoxidized either by charge recombination with the oxidized dimer or by an external oxidizing agent. The two possibilities are kinetically well separated (Figures 6 and 7). In addition to mediators if available (*52*), oxygen or the pool of quinones can serve as an electron acceptor for Q_A^- or Q_B^- (data not shown). At the relatively small pool size of quinones, the mole fraction of reoxidized Q_A^- by the external redox agent can be titrated according to a Nernst curve where the midpoint redox potential $E_m = 160$ mV (Figure 8).

From kinetic analysis of the contribution of the slow and very slow components of the P^+ dark relaxation after illumination of variable duration, the rate constants of Q_A^- reoxidation (k_Q) in the two conformation states of the RC were determined at different pH values for UQ_{10} and AQ at the Q_A binding site (Figure 9). The pH dependence of the rate constants showed a similar pattern, indicating that both processes are controlled by protonation of similar protonatable groups of the protein. Due to the significant difference in midpoint redox potentials of the quinones [$E_m = -50$ mV (UQ_{10}) and $E_m = -210$ mV (AQ) at pH 8; *53*], the rates for AQ are much higher than those for UQ_{10}. The ratio in semiquinone reoxidation rates can be as large as 3 orders of magnitude at pH 6.

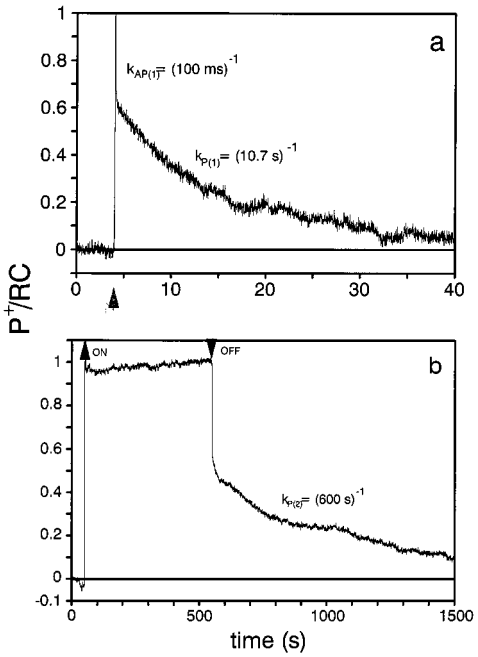

FIGURE 7: Kinetics of the disappearance of the light-induced P^+Q_A state measured at 865 nm in two conformation states of the RC at pH 6.0. The first conformation was achieved after flash excitation and fast dark relaxation [$k_{AP(1)} = (100\ ms)^{-1}$] at a relatively high *in situ* redox potential ($E_h = 400$ mV) (panel a). The second conformation was obtained after a prolonged (500 s) and strong (1 W cm^{-2}) illumination and fast dark relaxation at an *in situ* redox potential E_h of 200 mV (panel b). Conditions were as follows: 3.0 μM RC and 500 μM $K_3[Fe(CN)_6]$ (a) or 2.5 μM RC (b), 0.03% Triton X-100, and 100 mM NaCl.

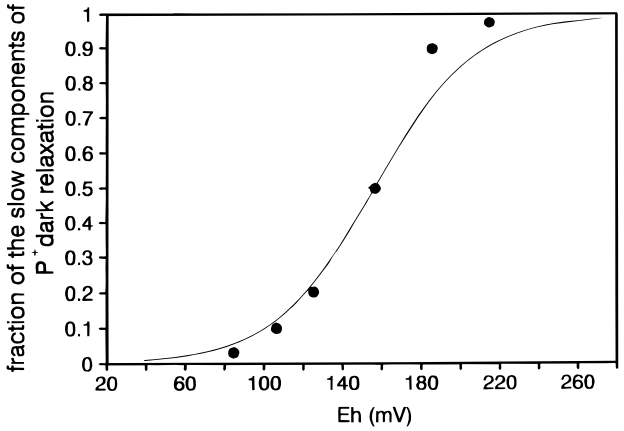

FIGURE 8: Fraction of the slow components of the P^+ dark relaxation as a function of the *in situ* redox potential. The (dark) relaxation of the oxidized dimer after a prolonged (100 s) illumination was monitored optically at 865 nm. The fast component was attributed to charge recombination, and all the slower phases were attributed to reoxidation of light-induced Q_A^-. Conditions were as follows: 2 μM RC, pH 6.0, 0.03% Triton X-100, 100 mM NaCl, and 10 μM PMS, DMBQ, and TMPD, depending on the E_h.

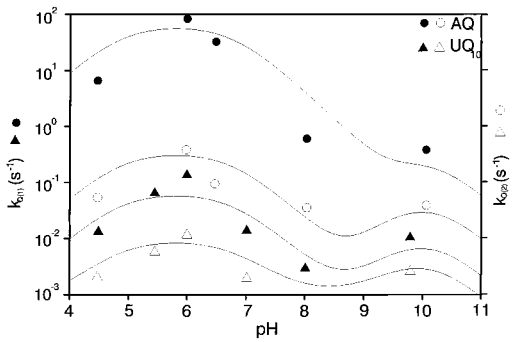

FIGURE 9: pH dependence of the rate constants of the semiquinone reoxidation in the two conformational states of the RC with native UQ_{10} and substituted AQ in the Q_A-binding site. The rate constants were determined from a series of P^+ dark relaxation kinetics after illumination with an increasing duration (see Figure 6a). The kinetic evaluations of the amplitudes of the slow [$k_{P(1)} = (10\ s)^{-1}$] and very slow [$k_{P(2)} = (600\ s)^{-1}$] components are attributed to the reoxidation of Q_A^- in the first and second conformation of the RC, respectively. The sum of observed rate constants weighted by mole fraction of five substates connected by p*K* values of 4.8, 6.8, 9.6, and 10.4 (see Scheme 1) are represented by solid lines. Conditions are the same as in Figure 3.

DISCUSSION

In this study, we performed proton binding/unbinding measurements on bacterial RCs exposed to strong and continuous illumination. The RC could not turn over because external electron donors to P^+ were not available. The motivation for such a study came from observation of a large proton release at acidic pH that was not found in flash-induced measurements earlier (*26*−*28*, *34*). The discussion will focus on the following questions: whether these protons come from RCs, what the precursor of the large proton release state of the RC is, and what minimal model of RC can account for the observed pH and E_h dependence of reoxidation of the semiquinone and deprotonation of the RC.

After flash excitation, the light-induced redox species P^+ and Q_A^- disappear simultaneously by charge recombination with a rate constant k_{AP} of 10 s^{-1} in Q_A active RCs. Strong and continuous illumination, however, holds the RC in a charge-separated state; therefore, P^+ and Q_A^- are exposed to external redox agents for longer periods of time. Under our redox conditions, Q_A^- is reoxidized much faster (k_Q) than P^+ is rereduced (k_P); thus, the RC can be trapped effectively in the P^+Q_A state. Under special conditions (high E_h and pH 6), where Q_A^- was rapidly oxidized by ferricyanide while the rereduction of P^+ by ferrocyanide remained slow, the P^+Q_A state could be achieved even after flash excitation and a substoichiometric amount of proton release was observed (*26*). Here, the P^+Q_A state was established by intense and continuous excitation, and large proton release was observed at pH 6 (Figure 1a). Independent measurements with pH indicator dyes and pH electrodes showed that the appearance (light on) and disappearance (light off) of the large proton release were correlated with the kinetics of the P^+Q_A state of the RC monitored by the very slow [$k_{P(2)}$] component of P^+ decay (Figures 1a and 7b). These data argue that the P^+Q_A state of the RC is a precursor of the observed large proton release.

Due to the long illumination and quantitatively small amount of proton release (10−20 μM), one can imagine that the protons originate not from the RC but from redox reactions related to rereduction of P^+ by an unidentified protonated donor, DH in the bulk: $DH + P^+ \rightarrow D + P + H^+$. This possibility, however, can be discounted on the basis of several observations. Quinone substitution (AQ for UQ_{10}) modified dramatically the kinetics of proton release and reoxidation of the semiquinone, although the redox reaction around the dimer was not affected at all (Figures 5 and 9). Differences in Q_B occupancy caused minor and characteristic changes in the pH dependence of proton stoichiometry (Figure 3). The pattern of proton release was not sensitive to redox mediators (PMS, DMBQ, and TMPD) which established the actual redox potential of the bulk and could serve as potential candidates for the electron donor donating to P^+. The pH dependence of the proton release was found to be characteristic of the protonatable amino acids available in the protein (Figures 3 and 10). This evidence shows that the observed H^+ ions were produced by the RC and not by redox reactions.

The experimental observations for the Q_A active RC can be interpreted in the frame of a minimal model where the RC after charge separation can turn from a dark-adapted conformation (1) to a light-adapted one (2) (Scheme 1). The two conformations differ strongly in their rate constants of the photochemistry (k_I, Figure 6b), reoxidation of the semiquinone (k_Q, Figure 9), and rereduction of the oxidized dimer (k_P, Figure 6a). In general, the rates in the light-adapted state are 1−2 orders of magnitude smaller than those in the dark-adapted state. We had no direct evidence of similar changes in charge back-reaction (k_{AP}). The rate of change in the conformation from 1 to 2 could be estimated by measurement of $k_c + k_{AP}$ if UQ_{10} (Figure 6a) and AQ are in the Q_A binding site (data not shown). In both cases, the rate of conformational change was at least comparable with that of the back-reaction. However, the rate of recovery (k_{-c}) was very small which can account for different phenomena observed during subsequent illuminations (Figure 6b; *54*).

The reoxidation of Q_A^- and the conformational change are reversible reactions, and the equilibrium constants (K_Q and K_c) and the rates (k_Q and k_c) depend on the E_h and pH of the solution. For the restricted E_h and pH range, similar conclusions were drawn by Shopes and Wraight (*55*) in RCs from *Rhodopseudomonas viridis*. K_Q for UQ_{10} in the Q_A pocket could be titrated on the redox scale (Figure 8). The significant difference in redox midpoint potentials between AQ and UQ_{10} explains the observed shift in rates (Figure 9) and equilibrium constants (Figure 7a, data not shown for AQ). The pH dependence of these parameters reveals what residues of the protein facilitate the reoxidation of the semiquinone, the conformational change, and the formation of the large proton release state. These processes are under the control of similar groups as their pH dependences have a similar pattern (Figures 3 and 9). While protonation/deprotonation of acidic groups has a large influence, basic residues have only a minor effect on the conformation change. Residues close to neutral pH, however, have no effect at all. The strength of control on semiquinone reoxidation and the conformational change may correlate with the number of protonatable residues in the cytoplasmic and periplasmic sides of the protein. The number of carboxylic acids (47 cytoplasmic + 12 periplasmic Glu and Asp) outweighs the number of tyrosines (18 + 10) and lysines (19 + 3) and even better the number of (not ligated) histidines (10 + 2) and cysteines (5 + 0) (*3*, *4*). Although the pattern of the change in ionization (ΔQ) of these residues

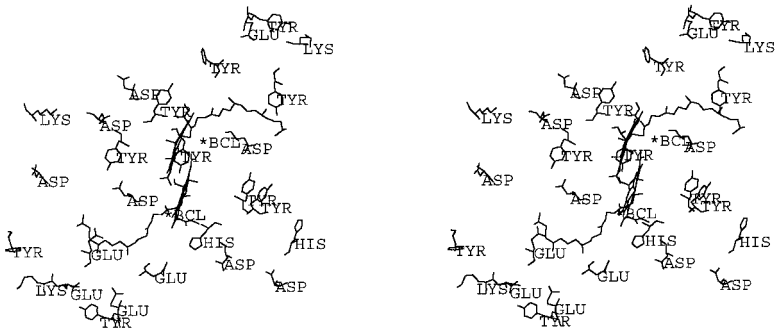

FIGURE 10: Stereoview of the protonatable amino acids around the dimer at the periplasmic side of the membrane looking from the top of the RC of *Rb. sphaeroides* (Ermler et al., 1994). Internal water molecules were omitted.

Scheme 1: Minimal Model for pH- and Conformation-Dependent Photochemistry and Subsequent Electron Transfer (Reoxidation of the Semiquinone and Rereduction of the Oxidized Dimer) and Protonation in Q_A Active RCs of *Rb. sphaeroides* at Room Temperature[a]

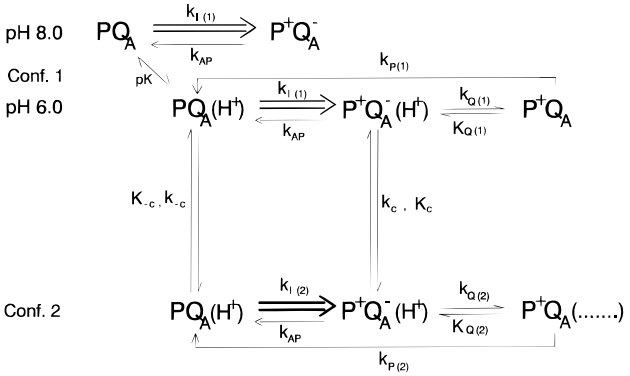

[a] The number of possible states is truncated to a characteristic unit corresponding to pH 8 and 6. No semiquinone reoxidation and no conformational change were considered at pH 8. The (pH- and E_h-dependent) rate constants and equilibrium constants of the reactions are denoted by *k* and *K*, respectively. Typical rate constants in native RC (UQ_{10} at the Q_A-binding site) at pH 6.0 are as follows: $k_{I(1)} = (2\ \text{ms})^{-1}$ and $k_{I(2)} = (5\ \text{s})^{-1}$ for photochemistry, $k_{AP(1)} = (100\ \text{ms})^{-1}$ for charge recombination, $k_{Q(1)} = (10\ \text{s})^{-1}$ and $k_{Q(2)} = (150\ \text{s})^{-1}$ for semiquinone reoxidation, $k_{P(1)} = (10\ \text{s})^{-1}$ and $k_{P(2)} = (600\ \text{s})^{-1}$ for rereduction of the oxidized dimer, $k_c + k_{AP(2)} \approx (150\ \text{ms})^{-1}$ for the upper limit of conformational change, and $k_{-c} \approx (6-8\ \text{h})^{-1}$ for complete relaxation of the sample. The numbers in parentheses correspond to one of the two conformational states of the RC.

as a function of pH [d*Q*/d(pH)] is subject to uncertainties of the actual pK_a values of the groups, it looks very similar to the curve directly measured for protonation (Figure 3).

Proton unbinding can be observed after reoxidation of the semiquinone. The kinetics showed two distinct phases (Figure 2). The slower and substoichiometric proton release can be attributed to formation of the P^+Q_A in the dark-adapted conformation which was already detected in earlier experiments (*26*, *28*). The much larger proton release comes from a similar redox state but a different (light-adapted) conformation of the RC. The new conformation of the protein opens the way for stronger (electrostatic) interaction of P^+ with the protonatable groups of the RC. These amino acids at the periplasmic side of the RC can be seen in Figure 10. The stoichiometry of proton release is limited not only by the number of available protonatable groups but also by the energetic coupling of the residues; the interaction with groups already deprotonated will decrease the p*K* shift of the unprotonated residues. The conservation law of the export of charges restricts the proton release from the RC. The loss of positive charge at the protonated residue upon deprotonation, however, can be screened by external ions. The outward movement of positive charges (H^+ ions) can be compensated for by inward movement of cations from the ionic cloud. The larger ionic strength of the solution should support larger proton release which is demonstrated by salt titration experiments of the proton release (Figure 2b).

We conclude that the observed high proton release is connected to a conformational switch which is controlled by the ionization states of the protonatable residues of the RC; the control is strong in the acidic pH range, weaker in the highly alkaline pH range, and very weak in the neutral pH region. In the high-proton release conformation state, the RC protein exposes several buried and/or ligated groups around the oxidized dimer to the bulk. The significance of exposure of partly buried protonatable groups in proton binding kinetics has been discussed recently (*56*). The interaction between P^+ and the protonatable groups and consequently the stoichiometry of proton release are controlled by the ionic strength of the solution.

The simple law of superposition of protonation due to different redox (and conformation) states of the RC is impaired. Whereas after flash excitation only a couple of protonatable groups are involved in proton uptake (or release) and the law of superposition is valid (*13*, *28*), under strong and continuous illumination, all groups become involved in protonation with no kinetic and/or accessibility limitations (*41*). As different redox states of the RC correspond to different conformations, the law of superposition of protonation due to different redox states (P^+Q_A, PQ_A^-, and $P^+Q_A^-$) will not be valid anymore: $\Delta H^+(P^+Q_A) + \Delta H^+(PQ_A^-) \neq \Delta H^+(P^+Q_A^-)$.

ACKNOWLEDGMENT

Thanks are due to Drs. Pierre Sebban (CNRS CGM, Gif-sur-Yvette, France) and Anthony Crofts and Colin A. Wraight (University of Illinois, Urbana, IL) for valuable discussions.

REFERENCES

1. Chang, C.-H., Tiede, D., Tang, J., Smith, U., Norris, J., and Schiffer, M. (1986) *FEBS Lett. 205*, 82−86.
2. Arnoux, B., Gaucher, J. F., Ducruix, A., and Reiss−Husson, F. (1995) *Acta Crystallogr. D 51*, 368−379.
3. Allen, J. P., Feher, G., Yeates, T. O., Komiya, H., and Rees, D. C. (1987) *Proc. Natl. Acad. Sci. U.S.A. 84*, 6162−6166.
4. Ermler, U., Fritzsch, G., Buchanan, S. K., and Michel, H. (1994) *Structure 2*, 925−936.

5. Arlt, T., Schmidt, S., Kaiser, W., Lauterwasser, C., Meyer, M., Scheer, H., and Zinth, W. (1993) *Proc. Natl. Acad. Sci. U.S.A. 90*, 11757−11761.
6. Woodbury, N. W., Becker, M., Middendorf, D., and Parson, W. W. (1985) *Biochemistry 24*, 7516−7521.
7. Kirmaier, Ch., and Holten, D. (1987) *Photosynth. Res. 13*, 225−260.
8. Kleinfeld, D., Okamura, M. Y., and Feher, G. (1984a) *Biochim. Biophys. Acta 766*, 126−140.
9. Vermeglio, A., and Clayton, R. K. (1977) *Biochim. Biophys. Acta 461*, 159−165.
10. Tiede, D. M., Vázquez, J., Córdova, J., and Marone, P. A. (1996) *Biochemistry 35*, 10763−10775.
11. Okamura, M. Y., and Feher, G. (1992) *Annu. Rev. Biochem. 61*, 861−896.
12. Okamura, M. Y., and Feher, G. (1995) in *Advances in Photosynthesis, Anoxygenic Photosynthetic Bacteria* (Blankenship, R. E., Madigan, M. T., and Bauer, C. E., Eds.) Vol. 2, pp 577−594, Kluwer Academic Publishers.
13. Maróti, P. (1993) *Photosynth. Res. 37*, 1−17.
14. Shinkarev, V. P., and Wraight, C. A. (1993) in *The photosynthetic reaction center* (Deisenhofer, H., and Norris, J. R., Eds.) pp 193−255, Academic Press, New York.
15. Arata, H., and Parson, W. W. (1981) *Biochim. Biophys. Acta 636*, 70−81.
16. Malkin, S., Churio, M. S., Shochat, S., and Braslavsky, S. E. (1994) *J. Photochem. Photobiol., B 23*, 79−85.
17. Mauzerall, D. C., Gunner, M. R., and Zhang, J. W. (1995) *Biophys. J. 68*, 275−280.
18. Kleinfeld, D., Okamura, M. Y., and Feher, G. (1984b) *Biochemistry 23*, 5780−5786.
19. Brzezinski, P., Okamura, M. Y., and Feher, G. (1992) in *The Photosynthetic Bacterial Reaction Center II: Structure, Spectroscopy and Dynamics* (Breton, J., and Vermeglio, A., Eds.) pp 321−330, Plenum Press, New York and London.
20. Tiede, D. M., and Hanson, D. K. (1992) in *The Photosynthetic Bacterial Reaction Center II: Structure, Spectroscopy and Dynamics* (Breton, J., and Vermeglio, A., Eds.) pp 341−350, Plenum Press, New York and London.
21. Kálmán, L., Turzó, K., and Maróti, P. (1993) *Photosynthetica 28*, 185−194.
22. Brzezinski, P., and Andréasson, L.-E. (1995) *Biochemistry 34*, 7498−7506.
23. Abresch, E. C., Stowell, M. H. B., McPhillips, T. M., Rees, D. C., Soltis, S. M., and Feher, G. (1997) *Biophys. J. 72* (2), A8.
24. Müh, F., Rautter, J., and Lubitz, W. (1997) *Biochemistry 36*, 4155−4162.
25. Cramer, W. A., and Knaff, D. B. (1990) *Energy Transduction in Biological Membranes*, Springer-Verlag, New York.
26. Maróti, P., and Wraight, C. A. (1987) in *Progress in Photosynthesis Research* (Biggins, J., Ed.) Vol. II, pp 401−404, Martinus Nijhoff, Dordrecht, The Netherlands.
27. Maróti, P., and Wraight, C. A. (1988a) *Biochim. Biophys. Acta 934*, 314−328.
28. McPherson, P. H., Okamura, M. Y., and Feher, G. (1988) *Biochim. Biophys. Acta 934*, 348−368.
29. McPherson, P. H., Okamura, M. Y., and Feher, G. (1993) *Biochim. Biophys. Acta 1144*, 309−324.
30. Sebban, P., Maróti, P., and Hanson, D. K. (1995) *Biochimie 77*, 677−694.
31. McPherson, P. H., Okamura, M. Y., and Feher, G. (1990) *Biochim. Biophys. Acta 1016*, 289−292.
32. Osváth, Sz., and Maróti, P. (1997) *Biophys. J. 73*, 972−982.
33. Graige, M. S., Paddock, M. L., Bruce, J. M., Feher, G., and Okamura, M. Y. (1996) *J. Am. Chem. Soc. 118*, 9005−9016.
34. Maróti, P., and Wraight, C. A. (1988b) *Biochim. Biophys. Acta 934*, 329−347.
35. Wraight, C. A. (1979) *Biochim. Biophys. Acta 548*, 309−327.
36. Maróti, P., Hanson, D. K., Schiffer, M., and Sebban, P. (1995) *Nat. Struct. Biol. 2* (12), 1057−1059.
37. Shinkarev, V. P., Takahashi, E., and Wraight, C. A. (1992) in *The Photosynthetic Bacterial Reaction Center II: Structure, Spectroscopy and Dynamics* (Breton, J., and Vermeglio, A., Eds.) pp 375−387, Plenum Press, New York and London.
38. Maróti, P. (1991) *Photosynthetica 25* (2), 173−180.
39. McMahon, B., Müller, J. D., Wraight, C. A., and Nienhaus, G. U. (1997) *Biophys. J. 72*, A418.
40. Fabian, M., Chamorovsky, S. K., Zakharova, N. I., Selivanov, V. A., and Kononenko, A. A. (1981) *Mol. Biol. (USSR) 15* (2), 439−446.
41. Kálmán, L., Gajda, T., Sebban, P., and Maróti, P. (1997) *Biochemistry 36*, 4489−4496.
42. Beroza, P., Fredkin, D. R., Okamura, M. Y., and Feher, G. (1992) in *The Photosynthetic Bacterial Reaction Center II: Structure, Spectroscopy and Dynamics* (Breton, J., and Vermeglio, A., Eds.) pp 363−374, Plenum Press, New York and London.
43. Beroza, P., Fredkin, D. R., Okamura, M. Y., and Feher, G. (1995) *Biophys. J. 68*, 2233−2250.
44. Gunner, M. R., and Honig, B. (1991) *Proc. Natl. Acad. Sci. U.S.A. 88*, 9151−9155.
45. Gunner, M. R., and Honig, B. (1992) in *The Photosynthetic Bacterial Reaction Center II: Structure, Spectroscopy and Dynamics* (Breton, J., and Vermeglio, A., Eds.) pp 403−410, Plenum Press, New York and London.
46. Lancaster, C. R. D., Michel, H., Honig, B., and Gunner, M. R. (1996) *Biophys. J. 70*, 2469−2492.
47. Stein, R. R., Castellvi, A. L., Bogacz, J., and Wraight, C. A. (1984) *J. Cell. Biochem. 25*, 243−259.
48. Okamura, M. Y., Isaacson, R. A., and Feher, G. (1975) *Proc. Natl. Acad. Sci. U.S.A. 72*, 3491−3495.
49. Liu, B.-L., Yang, L.-H., and Hoff, A. J. (1991) *Photosynth. Res. 28*, 51−58.
50. Dutton, P. L. (1978) *Methods Enzymol. 54*, 411−435.
51. Okamura, M. Y., Isaacson, R. A., and Feher, G. (1979) *Biochim. Biophys. Acta 546*, 394−417.
52. Mulkidjanyan, A. Ya., Shinkarev, V. P., Verkhovsky, M. I., and Kaurov, B. S. (1986) *Biochim. Biophys. Acta 849*, 150−161.
53. Woodbury, N. W., Parson, W. W., Gunner, M. R., Prince, R. C., and Dutton, P. L. (1986) *Biochim. Biophys. Acta 851*, 6−22.
54. Goushcha, A. O., Kharkyanen, V. N., and Holzwarth, A. R. (1997) *J. Phys. Chem. B 101*, 259−265.
55. Shopes, R., J., and Wraight, C. A. (1986) *Biochim. Biophys. Acta 848*, 364−371.
56. Maróti, P., and Wraight, C. A. (1997) *Biophys. J. 73*, 367−381.

BI971882Q